Analysis of Multipactor RF Breakdown in a Waveguide Containing a Transversely Magnetized Ferrite

Daniel González-Iglesias, Álvaro Gómez, Benito Gimeno, *Member, IEEE*, Óscar Fernández, Angel Vegas, *Member, IEEE*, Fernando Casas, Sergio Anza Hormigo, Carlos Vicente, *Member, IEEE*, Jordi Gil, Rafael Mata, Isabel Montero, Vicente E. Boria, *Senior Member, IEEE*, and David Raboso

***Abstract*— In this paper, the multipactor RF breakdown in a parallel-plate waveguide partially filled with a ferrite slab magnetized normal to the metallic plates is studied. An external magnetic field is applied along the vertical direction between the plates in order to magnetize the ferrite. Numerical simulations using an in-house 3-D code are carried out to obtain the multipactor RF voltage threshold in this kind of structures. The presented results show that the multipactor RF voltage threshold at certain frequencies becomes considerably lower than for the corresponding classical metallic parallel-plate waveguide with the same vacuum gap.**

***Index Terms*— Ferrite devices, magnetic field, multipactor effect, parallel-plate waveguide, RF breakdown.**

I. Introduction

MULTIPACTOR discharge is an undesired phenomenon that takes place on devices operating under vacuum conditions and high-power RF electromagnetic fields [1], [2]. When certain conditions arise, free electrons in the device are driven by the RF electric field toward the walls. If the kinetic energy of the impacting electrons is high enough, secondary electrons may be released from the surface. As a consequence, a chain reaction leading to an exponential growth of the electron population inside the component is started. The onset of the multipactor discharge degrades the device performance by several negative effects, such as increasing the signal noise and reflected power, heating up the device walls, outgassing, detuning of resonant cavities, vacuum window failure, and even resulting in the total destruction of the component. Due to that, multipactor phenomenon is revealed as a crucial limitation in the maximum RF power handling. Multipactor occurs in different environments, such as passive components of satellite communication payloads, particle accelerators, and klystrons.

Special attention must be paid to multipactor in satellite components, where replacement of damaged devices is not possible. Therefore, in order to ensure that the RF component will not suffer this undesirable phenomenon during operation, it is extremely important to take into account this effect in the design process. In fact, restrictive specifications have been imposed by the space agencies about this issue [3].

Multipactor has been extensively analyzed in the case of metallic surfaces so far [4], [5], [6]. Recently, some studies have focused their attention to the case wherein dielectric surfaces are involved [7], [8], [9]. However, very little literature about multipactor effect in devices containing ferrites can be found [10], [11]. Ferrites are ferromagnetic materials which exhibit magnetic anisotropy when are brought under a dc magnetic bias field. When an external dc magnetic field is applied multipactor discharge can be either suppressed [12] or enhanced [13], depending on the specific magnitude and direction of the external field. The induced anisotropy in the ferrite has been used to produce a wide range of RF passive devices, such as circulators, isolators, and phase shifters [14]–[17]. Until now, the high power handling of this kind of components can only be analyzed by rough approximations whose validity is not clear.

The main aim of this paper is the study of the multipactor effect in an ideal uniform parallel-plate waveguide (as shown in Fig. 1) of infinite length along the x- and z-axes, z being the propagation direction of the electromagnetic wave,

Manuscript received May 13, 2016; revised August 3, 2016; accepted September 22, 2016. Date of publication October 13, 2016; date of current version November 22, 2016. This work was supported in part by the European Space Agency under Novel Investigation in Multipactor Effect in Ferrite and other Dielectrics used in high power RF Space Hardware under Contract AO 1-7551/13/NL/GLC, in part by the Spanish Government under Coordinated R&D Project TEC2013- 47037-5-R and Project TEC2014-55463-C3-3-P, and in part by the European Commission (ERDF). The review of this paper was arranged by Editor R. Carter.

D. González-Iglesias, B. Gimeno, and R. Mata are with the Departamento de Física Aplicada, Universidad de Valencia, 46100 Valencia, Spain (e-mail: daniel.gonzaleziglesias@uv.es; benito.gimeno@uv.es; rafael.mata@uv.es).

Á. Gómez, Ó. Fernández, and A. Vegas are with the Departamento de Ingeniería de Comunicaciones, Universidad de Cantabria, 39005 Santander, Spain (e-mail: alvaro.gomez@unican.es; oscar.fernandez@unican.es; angel.vegas@unican.es).

F. Casas is with the Instituto Universitario de Matemáticas y Aplicaciones, Universidad Jaume I, 12071 Castellón de la Plana, Spain (e-mail: casas@uji.es).

S. Anza Hormigo, C. Vicente, and J. Gil are with AURORASAT, 46001 Valencia, Spain (e-mail: sergio.anza@aurorasat.es; carlos.vicente@aurorasat.es; jordi.gil@aurorasat.es).

I. Montero is with the Instituto de Ciencia de Materiales de Madrid, Consejo Superior de Investigaciones Científicas, 28049 Madrid, Spain (e-mail: imontero@icmm.csic.es).

V. E. Boria is with the Departamento de Comunicaciones, Instituto de Telecomunicaciones y Aplicaciones Multimedia, Universidad Politécnica de Valencia, 46022 València, Spain (e-mail: vboria@dcom.upv.es).

D. Raboso is with the European Space Research and Technology Centre, European Space Agency, 2201 AZ Noordwijk, The Netherlands (e-mail: david.raboso@esa.int).

Digital Object Identifier 10.1109/TED.2016.2614370

0018-9383 © 2016 IEEE. Personal use is permitted, but republication/redistribution requires IEEE permission.
See http://www.ieee.org/publications_standards/publications/rights/index.html for more information.

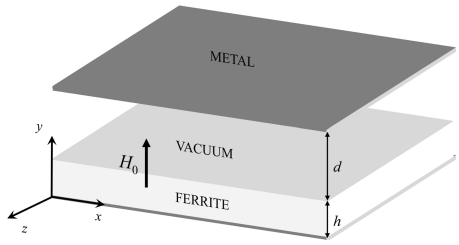

Fig. 1. Parallel-plate waveguide (considered to be infinite along the x- and z-axes, z being the propagation direction of the electromagnetic wave) partially loaded with a ferrite slab magnetized along the waveguide gap direction by a static magnetic field $\vec{H}_0$.

thus resulting an electromagnetic field which does not depend on the x-coordinate. Transmission of the fundamental TEM like mode is considered in this analysis. The waveguide contains a lossless ferrite slab, which is magnetized along the direction perpendicular to the metallic walls, i.e., $\vec{H}_0 = H_0\,\hat{y}$. When the ferrite is saturation magnetized, it can be electromagnetically characterized by the constitutive relations $\vec{D} = \varepsilon\vec{E}$ and $\vec{B} = [\mu]\vec{H}$, wherein ε is the dielectric permitivitty and $[\mu]$ is the Polder's tensor corresponding to the aforementioned magnetization [14, eq. 9.27]. The effective field $H_{\rm ef}$ which magnetizes the ferrite is $H_{\rm ef} = H_0 - M_s$ [14], where M_s is the saturation magnetization. There is a gyromagnetic resonance of the ferrite at the Larmor frequency $\omega_0 = \gamma\,\mu_0 H_{\rm ef}$, where μ_0 is the free space permeability, and $\gamma = e/m$ is the gyromagnetic ratio of the electron ($-e$ and m are the electron charge and electron mass at rest, respectively).

In a previous authors' work [11], which at first glance could be seen similar to the current one, the external magnetization field was oriented parallel to the ferrite slab. Since the magnetic permeability of the ferrite is anisotropic and depends on the bias magnetic field H_0 direction, the RF behavior of the ferrite in both cases is completely different. Moreover, the effect on the electron orbits due to changing the direction of the external magnetic field employed to magnetize the ferrite is crucial. Therefore, the present analysis is not only a straightforward extension of the previous one, and it is worthy of being studied.

This paper is structured as follows. First, in Section II, it is described both the multipactor algorithm and the method employed to compute the RF electromagnetic fields in such ferrite loaded waveguide. Next, Section III presents and analyzes the results of the multipactor simulations. Finally, the main conclusions of our study are summarized in Section IV.

II. Theory

A. Multipactor Algorithm

The simulation code developed for the study of the multipactor is based on the single effective electron model [4]. This method consists of tracking the individual trajectories of a set of effective electrons. Each effective electron has associated a cumulative electron population that takes into account the emission or absorption of secondary electrons by the device walls. This is done by computing the value of the secondary electron yield (SEY) function (δ) at each impact, which depends on the electron kinetic energy and impacting angle [18], [19]. After the impact, the colliding effective electron is launched back to the waveguide with random velocity given by a Maxwellian distribution with a mean certain kinetic energy (3 eV in our simulations). The velocity angle follows the cosine law distribution [20]. When the software has run for a predefined number of RF periods, the code stops and the time evolution of the total electronic population is shown.

The individual trajectories of the effective electrons are computed by solving numerically their nonrelativistic equations of motion derived from the Lorentz Force. The total electromagnetic field experienced by the electron is the superposition of the RF electric $E_{\rm RF}$ and magnetic $B_{\rm RF}$ fields, the electric field due to the space charge effect $E_{\rm sc}$, the dc electric field appearing because of the charging of the ferrite surface $E_{\rm dc}$, and the external magnetic field H_0 employed to magnetize the ferrite. Both $E_{\rm sc}$ and $E_{\rm dc}$ have been computed following the procedure reported in [7].

For the numerical integration of the differential equations of the electron trajectories, we use a conveniently modified velocity-Verlet method. This particular scheme has very favorable properties concerning the error propagation in time, both in the energy and the position and velocity. We choose the time step size so that the relative error in position and in energy is less than 1% after a time of 200 RF periods.

B. RF Electromagnetic Field Computation

The RF electromagnetic field inside the structure under study has been obtained with the aid of the coupled mode method (CMM). This well-known numerical method, formulated in the frequency domain, has been widely and successfully used in the analysis of the electromagnetic wave propagation inside uniform waveguides that contain any isotropic, anisotropic, or complex material [21], [22], [23].

In few words, the CMM is a method of moments, which consists on expanding the electromagnetic field components inside the structure under analysis in terms of a set of base functions previously defined [21]. In many cases, these base functions correspond to the electric or magnetic field components of the TE and TM modes of the empty waveguide. Therefore, they are called basis modes. According to this idea, any component of the electromagnetic field of the structure under test can be expressed as a linear combination of the basis modes.

Once the electromagnetic fields inside the waveguide are obtained, the calculation of the equivalent voltage V_0 is done by integrating the vertical RF electric field along the vacuum gap.

III. Simulations

In order to compute the multipactor RF voltage threshold for the parallel-plate ferrite loaded waveguide shown in Fig. 1, numerical simulations have been performed. For all the considered cases, the ferrite thickness h and the vacuum gap d have been selected to match with the height of a WR-90 rectangular waveguide, i.e., $b = d + h = 10.16$ mm. The saturation

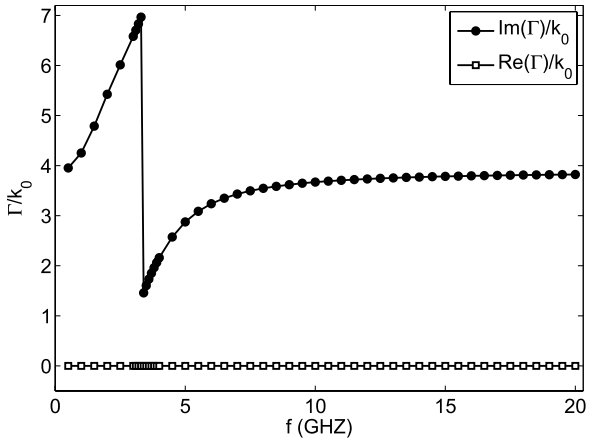

Fig. 2. Real and imaginary parts of the propagation factor for the fundamental mode of a ferrite loaded waveguide (with $d = 1$ mm) as a function of the RF frequency. Note that gyromagnetic resonance, given by Larmor frequency, occurs at 3.34 GHz.

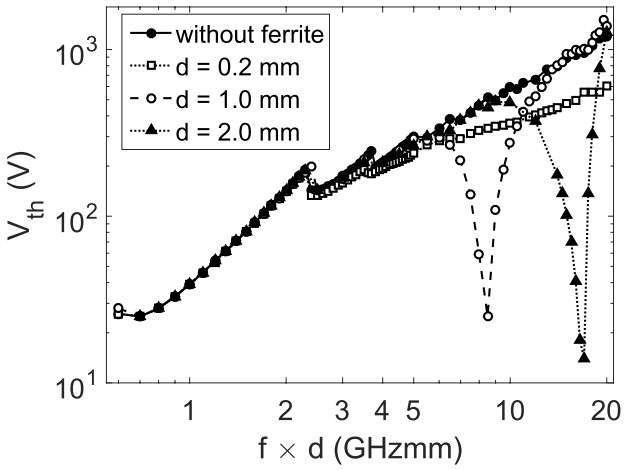

Fig. 3. Multipactor RF voltage threshold as a function of the frequency gap. Results are presented for parallel-plate ferrite loaded waveguides with different gap lengths and ferrite thicknesses (but maintaining the height of a WR-90 waveguide), and also for a metallic parallel-plate waveguide ("without ferrite").

magnetization of the ferrite is $4\pi M_s = 1806$ G, its relative dielectric permittivity $\varepsilon_r = 15$, and its SEY parameters are: first crossover energy for SEY coefficient equal to unity, $W_1 = 19$ eV, maximum SEY coefficient $\delta_{\max} = 2.88$, and impact kinetic energy for $\delta_{\max}$, $W_{\max} = 289$ eV [24]. For simplicity, the same SEY parameters are selected for the top metallic wall. The external magnetic field employed to magnetize the ferrite is $H_0 = 3000$ Oe. Consequently, the effective biasing field inside the ferrite is $H_{\text{ef}} = 1194$ Oe. The considered fields are those corresponding to the fundamental mode of the ferrite loaded waveguide (i.e., $l = 1$). For all calculations of the electromagnetic field components with the CMM, a total number of 75 TE and 75 TM basis modes are used. These basis modes have been included by increasing their cutoff frequencies.

We are interested in analyzing the effect of the variation of the ferrite thickness and the vacuum gap length in the multipactor RF voltage threshold. First, for the fundamental mode, the propagation factor dependence with frequency it is obtained, as shown in Fig. 2. It can be observed that the real part of the propagation factor is zero within the plotted frequency range, which corresponds to a propagative mode.

In Fig. 3, the variation of the multipactor RF voltage threshold as a function of the frequency gap value (i.e., the multipactor susceptibility chart) is shown for several ferrite loaded parallel-plate waveguides. Note that for each curve, the gap remains fixed. Moreover, the results for a classical metallic parallel-plate waveguide with no ferrite slab, a gap of $d = 0.2$ mm and $H_0 = 0$ (henceforth referred as without ferrite case) has been included for comparison purpose. Remember that according to the well-known multipactor theory [2] for a classical metallic parallel-plate waveguide, the multipactor phenomenon depends only on the frequency gap product, and as a consequence, the same multipactor RF voltage threshold curve would be obtained for metallic parallel-plate waveguides with other gaps while maintaining the same frequency gap range. From the results (recall Fig. 3), it is noticed that there is considerable difference between the multipactor RF voltage threshold of the ferrite loaded waveguides and the corresponding to the without ferrite case. It is found that this discrepancy increases with the gap value. In fact, the maximum difference in the multipactor RF voltage threshold between the $d = 0.2$ mm waveguide and the without ferrite case is of 6.5 dB, while in the $d = 1$ mm and $d = 2$ mm, the difference becomes of 26 and 37 dB, respectively. It is also observed that the multipactor behavior of the ferrite loaded waveguides remains very close to the without ferrite case for low-frequency gap values (below 2.5 GHzmm). In general terms, the multipactor RF voltage threshold of the ferrite loaded waveguide cases tends to be equal or below the without ferrite multipactor threshold.

In order to have a better understanding of the behavior of the different multipactor susceptibility curves, a detailed analysis of the RF electromagnetic fields (spatial distribution, scale analysis of the different electric, and magnetic spatial components), and electron dynamics (resonant trajectories and multipactor order) has been performed for both the ferrite loaded waveguides and the classical unloaded metallic parallel-plate waveguide.

An exhaustive inspection of the RF electromagnetic field pattern of the three ferrite loaded waveguide cases has revealed that the RF magnetic field has very little influence in the electron motion, and thus, the contribution of the terms $v_i\ B_{\text{RF},j}$ (being $i, j = x, y, z$) can be neglected in the differential equations of the electron motion. Regarding the RF electric field components, it has been found that all of them have noticeable effects in the electron trajectories. In Fig. 4 (left), it has been depicted the quotient between the maximum absolute value along the gap of the $E_{\text{RF},x}$ and $E_{\text{RF},y}$ components for the different considered ferrite waveguides. In a similar way in Fig. 4 (right), it has been plotted the same quotient for the $E_{\text{RF},z}$ and $E_{\text{RF},y}$ components. From these figures, it is extracted that the $E_{\text{RF},y}$ is the greater RF electric field component for low-frequency gap values. As the frequency

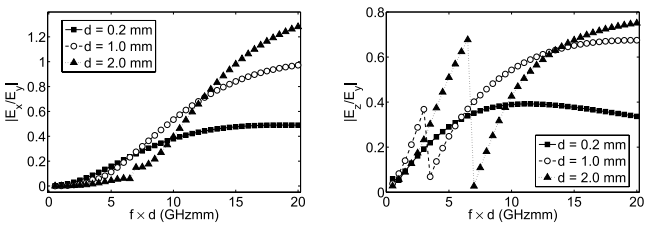

Fig. 4. Left (right): quotient between the maximum absolute value along the gap of the $E_{\mathrm{RF},x}$ ($E_{\mathrm{RF},z}$) and $E_{\mathrm{RF},y}$ components for the ferrite loaded waveguides.

gap increases the components, $E_{\mathrm{RF},x}$ and $E_{\mathrm{RF},z}$ also grow with regard to the $E_{\mathrm{RF},y}$ component. This increment is found to be more notorious for the ferrite loaded waveguides with higher gaps. In fact, it can be observed that $E_{\mathrm{RF},x}$ becomes the dominant component in the $d = 2$ mm waveguide for values above 15 GHz mm.

Taking the previous statements into account, the differential equations of motion can be approximated in the following way for the earlier stages of the electron multiplication:

$$\frac{dv_x}{dt} \simeq \omega_c v_z - \frac{e}{m} E_{\mathrm{RF},x} \cos(\omega t + \phi) \tag{1}$$

$$\frac{dv_y}{dt} \simeq -\frac{e}{m} E_{\mathrm{RF},y} \cos(\omega t + \phi) \tag{2}$$

$$\frac{dv_z}{dt} \simeq -\omega_c v_x - \frac{e}{m} E_{\mathrm{RF},z} \sin(\omega t + \phi) \tag{3}$$

where $E_{\mathrm{RF},x}$, $E_{\mathrm{RF},y}$, and $E_{\mathrm{RF},z}$ are the x, y, and z RF electric field components, respectively, which only depend on the y-coordinate; $\omega_c = (e/m)\mu_0 H_0$ is the cyclotron angular frequency, $\omega = 2\pi f$ is the RF angular frequency (f being the RF frequency), v_x, v_y, and v_z are the x-, y-, and z-components of the velocity vector, respectively, and ϕ is the phase of the RF electromagnetic field. It is remarkable that in such conditions, the equation of motion for the y-coordinate gets decoupled from the remaining x- and z-coordinates. Indeed, the approximated y-equation of motion becomes the corresponding one of the analytically well-studied classical case without ferrite [1], [2]. The effect of the external field H_0 is to spin the electron orbits in the xz plane. In addition, the $E_{\mathrm{RF},x}$ and $E_{\mathrm{RF},z}$ components accelerate the electron along the directions x and z, respectively. Manipulating the expressions (1) and (3), the following differential equations arise for the v_x and v_z velocities:

$$\frac{d^2 v_x}{dt^2} + \omega_c^2 \, v_x = A_1 \, \sin(\omega t + \phi) \tag{4}$$

$$\frac{d^2 v_z}{dt^2} + \omega_c^2 \, v_z = A_2 \, \cos(\omega t + \phi) \tag{5}$$

where $A_1 = (e/m)(E_{\mathrm{RF},x,0}\,\omega - E_{\mathrm{RF},z,0}\,\omega_c)$ and $A_2 = (e/m)$ $(E_{\mathrm{RF},x,0}\,\omega_c - E_{\mathrm{RF},z,0}\,\omega)$. The above differential equations can be solved analytically provided that the amplitude of the RF electric field components is uniform along the gap. Although this is not true in our case, we will take this assumption in order to obtain some analytical expressions that can give us a certain qualitative insight of the multipactor phenomenon. After some calculations, the following expressions arise for the v_x and v_z velocities (it is assumed zero initial velocity for both coordinates):

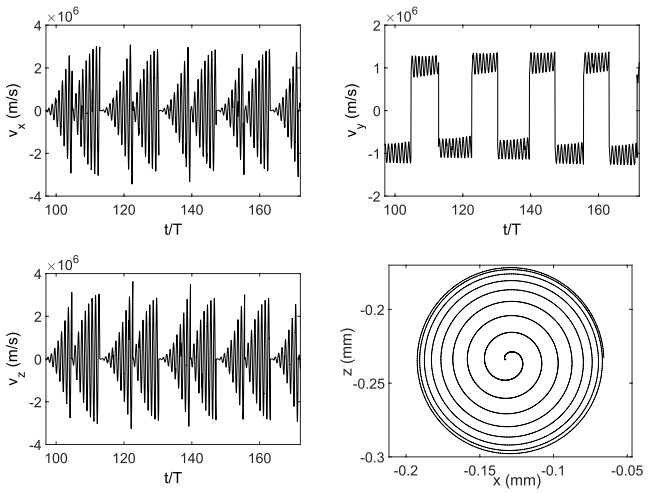

Fig. 5. From left to right, and up to down: effective electron velocity components as a function of the time normalized to the RF period (T is the RF period), and xz plane electron trajectory. All for a ferrite waveguide with $d = 1$ mm, $f \times d = 8.5$ GHzmm, $V_0 = 25$ V.

$$v_x = \frac{A_1}{\omega_c^2 - \omega^2} \sin(\omega t + \phi) - \frac{A_1 \, \sin(\phi)}{\omega_c^2 - \omega^2} \, \cos(\omega_c t) - \frac{A_2 \, \cos(\phi)}{\omega_c^2 - \omega^2} \, \sin(\omega_c t) \tag{6}$$

$$v_z = \frac{A_2}{\omega_c^2 - \omega^2} \cos(\omega t + \phi) - \frac{A_2 \, \cos(\phi)}{\omega_c^2 - \omega^2} \, \cos(\omega_c t) + \frac{A_1 \, \sin(\phi)}{\omega_c^2 - \omega^2} \, \sin(\omega_c t). \tag{7}$$

Note that (6) and (7) are valid for all the RF frequencies except for $\omega = \omega_c$. For both velocities, there are oscillatory terms at both the RF frequency and at the cyclotron frequency. It is easily noticed that the amplitude of these oscillations becomes maximum when the RF frequency equals the cyclotron one ($\omega = \omega_c$). Consequently, the velocity gain in the plane xz is maximum in the neighborhood of such resonance. In our case, the cyclotron frequency is 8.4 GHz and the corresponding frequency gap is 8.4 GHz mm for the $d = 1$ mm waveguide and 16.8 GHz mm for the $d = 2$ mm waveguide. This cyclotron resonance allows to understand the sharp minimums observed for the multipactor RF voltage thresholds of the ferrite loaded waveguides with $d = 1$ mm and $d = 2$ mm in the surroundings of such frequency gap values. Due to the enhance in kinetic energy gain of the electron in the xz plane, less RF voltage amplitude is necessary to achieve that the total kinetic impact energy of the electron exceeds the W_1 of the material. To illustrate the cyclotron resonance effect, in Fig. 5, we have plotted the v_x, v_y, and v_z velocities of an effective electron in the $d = 1$ mm ferrite loaded waveguide, for a frequency gap value close to the resonance and an RF voltage value corresponding to the multipactor threshold. It is noticed the increment of the v_x and v_z maximum amplitude in the successive oscillations between one impact and next, while for the v_y velocity, it is not observed such maximum

amplitude increment. In Fig. 5, it has also been depicted the xz plane electron trajectory, which seems very similar to that of a cyclotron accelerator, where the radius of the electron circular trajectory tends to increase as the kinetic energy gain process is ongoing.

The above statements justify the presence of a sharp minimum in the multipactor RF voltage threshold for the frequency gap values in the vicinity of the cyclotron resonances for the $d = 1$ mm and $d = 2$ mm ferrite loaded waveguide cases. However, it is notorious that such multipactor RF voltage threshold minimum is not observed for the $d = 0.2$ mm waveguide (which should be expected at 1.68 GHz mm). To understand this point, we will briefly recall some aspects of the classic multipactor theory for parallel-plate waveguides. As it is well known, for the onset of a multipactor discharge, it is required that the electron becomes synchronized with the RF electric field (it implies the apparition of stable resonant trajectories, also known as multipactor modes), and an electron impact kinetic energy with the waveguide walls above the W_1 parameter of the material (which ensures the release of secondary electrons). The classical multipactor modes that guarantee the electron synchronization with the RF electric field consist on electron trajectories that take an odd number of RF semiperiods to cross the gap (the multipactor order N is defined as that number of RF semiperiods).

In our ferrite loaded waveguide case, we have argued previously that the y motion becomes decoupled from the x- and z-coordinates, resulting in the same y differential equation of motion that for the classical metallic parallel-plate waveguide. The only difference in the y equation of motion between the unloaded ferrite waveguide and the ferrite waveguide is that, in the latter case, the $E_{\mathrm{RF},y}$ is inhomogeneous along the gap. However, we can take the assumption of spatial homogeneity as a first approach to our problem. When such consideration is done, we can use the classical multipactor modes and formulas to qualitatively explain the ferrite loaded waveguide. We will rely on two expressions to reach this aim. The first expression, $V_{0,\min}$, gives the minimum RF voltage that guarantees a resonant multipactor of order N. To deduce such equation we have imposed that an electron starting from $y = 0$ arrives to $y = d$ in a time $(NT/2$, then we have searched the starting phase of the RF field (ϕ) that gives the lowest RF value [1], [2]

$$V_{0,\min} = \frac{m}{e}\frac{(\omega d)(\omega d - v_{0y}\pi N)}{2\sqrt{1+\left(\frac{\pi N}{2}\right)^2}} \tag{8}$$

where v_{0y} is the y-component of the initial velocity. It must be remarked that the RF voltage calculated with (8) does not ensure that the kinetic energy due to v_y is above the W_1 parameter. The second expression is for the RF voltage that ensures a resonant multipactor mode of order N with an electron impacting with a kinetic energy of W_1, i.e., $V_{0,W1}$. In some cases, the values given by expressions of $V_{0,W1}$ or $V_{0,\min}$ may not correspond to valid resonant trajectories. The procedure to deduce $V_{0,W1}$ consists of imposing the two aforementioned conditions in the equations of the y trajectory and the v_y velocity. Finally, it is obtained that

$$V_{0,W_1} = \frac{m}{e}\frac{(\omega d)(\omega d - v_{0y}\pi N)}{\pi N \sin\phi_{W_1} - 2\cos\phi_{W_1}}$$
$$\phi_{W_1} = \operatorname{arc\,cot}\left(\frac{\pi N}{2} - \frac{\omega d - v_{0y}\pi N}{v_{iy}}\right) \tag{9}$$

where v_{iy} is the y impacting velocity that is set to match with the W_1 kinetic energy. Note that expressions (8) and (9) depend on the frequency gap product. For each frequency gap value, it can be estimated the minimum RF voltage at which each of the multipactor modes appears.

TABLE I
MULTIPACTOR MODES FOR $f \times d = 8.4$ GHz mm

N	V_{0,W_1} (V)	$V_{0,min}$ (V)	$W_{i,V_{0,min}}$ (eV)
1	7111	4043	1579
3	5487	1390	280
5	3864	743	95
7	2244	459	43
9	656	300	23
11	x	199	14
13	x	129	8.4
15	x	77	5.4
17	x	37	3.5
19	x	6	2.3

The first multipactor modes at a frequency gap value of 8.4 GHz mm are shown in Table I. The first column indicates the order of the multipactor mode N; second column gives the RF voltage to ensure the resonant electron impacts with a kinetic energy equal to the W_1 (19 eV in our case) of the material, V_{0,W_1}; third column provides the minimum RF voltage at which the resonant trajectories appear, $V_{0,\min}$, and fourth column is for the electron impact kinetic energy when the RF voltage is $V_{0,\min}$ and $W_{i,V_{0,\min}}$. If $W_{i,V_{0,\min}}$ is equal or above W_1 then $V_{0,\min}$ is the multipactor RF voltage threshold for the N mode, if not the multipactor RF voltage threshold is $V_{0,W1}$. At the view of the results summarized in Table I, the $N = 9$ multipactor mode appears at an RF voltage threshold lower than the other available modes ($N = 1, 3, 5, 7$), which appear at higher RF voltages than the multipactor threshold. Electron resonant trajectories with $N = 11, 13, 15, \ldots$ may appear but cannot contribute to the eventual onset of the discharge since their impacting energies are below W_1. The results of the multipactor numerical simulations for the without ferrite waveguide are in concordance with the theoretical predictions of Table I. Indeed, in Fig. 6 (left), it is depicted the effective electron vertical trajectory at 8.4 GHz mm in the multipactor RF voltage threshold, revealing the presence of a resonant multipactor with $N = 9$. In Fig. 6 (right), it is depicted the effective electron vertical trajectories at the same frequency gap in the multipactor RF voltage threshold for the ferrite loaded waveguide with $d = 1$ mm. Note that at this frequency gap, the cyclotron resonance occurs and the multipactor RF voltage threshold is clearly below the without ferrite value. For this case, it cannot be found a well-defined multipactor order, instead a hybrid multipactor than ranges from order

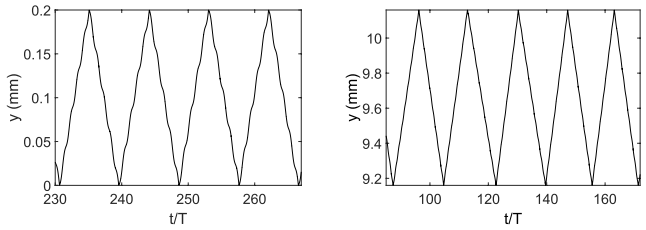

Fig. 6. Vertical coordinate effective electron trajectories as a function of the time normalized to the RF period, $f \times d = 8.4$ GHz mm. Left: metallic parallel-plate waveguide (without ferrite case), $V_0 = 518$ V. Right: ferrite loaded waveguide with $d = 1$ mm and $V_0 = 25$ V.

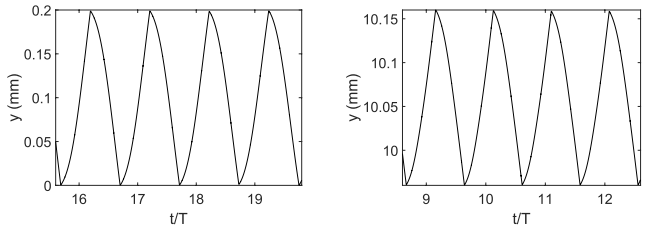

Fig. 7. Vertical coordinate effective electron trajectories as a function of the time normalized to the RF period, $f \times d = 1.68$ GHz mm. Left: metallic parallel-plate waveguide (without ferrite case), $V_0 = 104$ V. Right: ferrite loaded waveguide with $d = 0.2$ mm and $V_0 = 103$ V.

TABLE II
MULTIPACTOR MODES FOR $f \times d = 1.68$ GHz mm

N	V_{0,W_1} (V)	$V_{0,min}$ (V)	$W_{i,V_{0,min}}$ (eV)
1	162	126	55
3	x	15	5.2
5	x	11	0.7

15 to 19 appears [see Fig. 6 (right)]. According to Table I, for such multipactor modes, there are no RF voltages that give an impact kinetic energy of the electron equal or above the W_1 of the material. Although resonant trajectories can appear (when the RF voltage exceeds $V_{0,\min}$), their impacting energies are quite below the W_1 (5.4 and 3.5 eV for the multipactor orders 17 and 19, respectively). However, these impacting energies have been obtained for the classical metallic parallel-plate waveguide (without ferrite), where there is only vertical RF electric field that accelerates the electron along that spatial direction. In the ferrite loaded case, the RF electric fields in the transverse xz plane induce an acceleration, which is uncoupled from the vertical dynamics of the electron but contributes to its total kinetic energy. Indeed, after analyzing the different spatial contributions to the electron total kinetic energy, it is noticed that the xz plane contribution notoriously exceeds the vertical contribution (recall Fig. 5). This occurs because the xz plane acceleration is maximum at the frequency gap value that fits the cyclotron resonance. This fact allows to reduce the multipator RF voltage threshold in the ferrite case with regard to the without ferrite case, thus moving from a multipactor order 9 (without ferrite case) to a 17–19 multipactor order (ferrite case).

In the same way that for Table I, the first resonant modes for $f \times d = 1.68$ GHz mm are shown in Table II. At this frequency gap value, only the multipactor mode with $N = 1$ can contribute to the multipactor discharge in the unloaded ferrite waveguide. Resonant trajectories with orders 3 and 5 may exist, but their impacting energies are insufficient to release secondary electrons. In Fig. 7 (left), it is depicted the effective electron vertical trajectory at 1.68 GHz mm in the multipactor RF voltage threshold for the without ferrite case; it can be observed the presence of the predicted multipactor mode of order 1. In Fig. 7 (right), it is also shown the effective electron vertical trajectory at the same frequency gap value for the ferrite waveguide with $d = 0.2$ mm; it is noticed the presence of the same multipactor mode ($N = 1$) that in the without ferrite case. Although for the ferrite case the frequency gap value matches the cyclotron resonance, the other available multipactor modes ($N = 3$ and $N = 5$) have too short flight time between successive impacts with the device walls, preventing the energy gain in the xz plane due to the cyclotron resonance. This fact justifies that the multipactor RF voltage thresholds are equal in the loaded and unloaded ferrite cases.

As it is well stated in the classical multipactor theory, the number of multipactor modes available for a multipactor discharge grows as the frequency gap increases [2]. In the same way, the flight time between successive electron impacts rises up as the multipactor order does. Thus, low-frequency gap values imply low crossing gap times for the electrons. This fact justifies similarity in the multipactor RF voltage threshold between the ferrite waveguide and the without ferrite cases for the low-frequency gap values (remember Fig. 3). Despite the presence of the accelerating RF electric field in the xz plane, the contribution to the electron kinetic energy is quite low due to short transit time. However, when the frequency gap increases the flight time also does, allowing higher gain in the transverse plane kinetic energy, and so reducing the multipactor RF voltage threshold regarding the without ferrite case (recall Fig. 3).

Previously, we have analyzed ferrite waveguides with the vacuum gaps of 0.2, 1, and 2 mm, and a total height equal to the standard WR-90 waveguide. For completeness, we try a ferrite loaded waveguide with a gap of $d = 5$ mm. According to the above statements, for the frequency gap value that matches the cyclotron resonance (in this case 42 GHzmm), it is expected a sharp minimum in the multipactor RF voltage threshold. Indeed, the results from the numerical simulations for the multipactor RF voltage threshold in the $d = 5$ mm ferrite waveguide shown in Fig. 8 confirm this statement. It should be remarked that for a classical metallic parallel-plate waveguide, no multipactor discharge is expected at such high-frequency gap values at the RF voltage levels employed in the RF satellite telecommunication systems.

Finally, it has been analyzed the case of having different SEY coefficients for the ferrite and the metal surface. The SEY parameters for the ferrite remain the same that were described previously in this section, while the SEY coefficients for the metal are those from the ECSS silver [3], i.e., $W_1 = 30$ eV, $W_{\max} = 165$ eV, and $\delta_{\max} = 2.22$. In Fig. 9, it is shown the multipactor RF voltage threshold for the ferrite waveguide

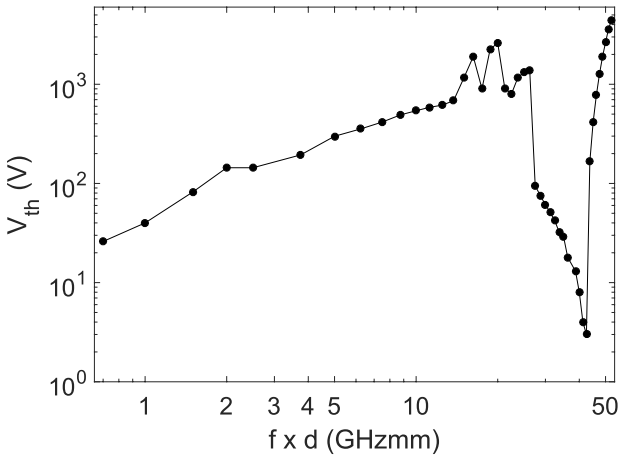

Fig. 8. Multipactor RF voltage threshold as a function of the frequency gap for a ferrite waveguide with $d = 5$ mm and $b = 10.16$ mm.

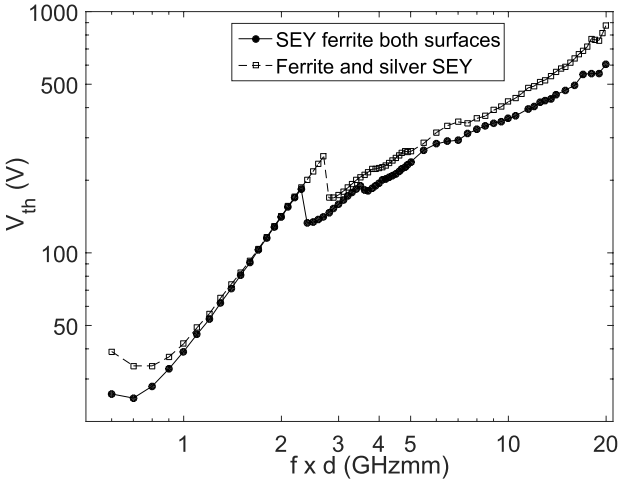

Fig. 9. Multipactor RF voltage threshold as a function of the frequency gap for a ferrite waveguide with $d = 0.2$ mm and $b = 10.16$ mm, considering the same SEY properties for both surfaces and considering different SEYs for ferrite and metal (silver) surfaces.

with $d = 0.2$ mm considering the ferrite and silver SEY properties, as well as the results considering the same SEY properties for both surfaces. It is observed slight differences between both cases. Note that the multipactor RF voltage threshold in the ferrite and silver SEY case tends to be greater than in the case with the same SEY in both surfaces, this is because the W_1 for silver is above the W_1 for the ferrite, and more RF voltage amplitude is required in the former case to reach the multipactor threshold.

IV. Conclusion

In this paper, the multipactor effect in a parallel-plate waveguide containing a magnetized ferrite slab has been studied. In order to magnetize the ferrite, an external static magnetic field oriented along the vertical direction was assumed. A home-made 3-D code based on the effective electron model was developed to carry out numerical simulations that allowed to compute the multipactor RF voltage threshold. The multipactor susceptibility charts obtained show that the multipactor RF voltage threshold changes with regard to the classical metallic parallel-plate situation with neither ferrite slab nor external magnetic field. In fact, a considerable reduction threshold with respect to the classic parallel-plate case has been found at some frequency gap ranges. Moreover, the analysis of the effective electron trajectories has led to a better understanding of the multipacting phenomenon in waveguides loaded with magnetized ferrites.

References

[1] J. Vaughan, "Multipactor," *IEEE Trans. Electron Devices*, vol. 35, no. 7, pp. 1172–1180, Jul. 1988.
[2] A. J. Hatch and H. B. Williams, "Multipacting modes of high-frequency gaseous breakdown," *Phys. Rev.*, vol. 112, no. 3, pp. 681–685, Nov. 1958.
[3] *Multipaction Design and Test*, document ECSS-E-20-01A, ESA-ESTEC, 2003.
[4] A. M. Pérez *et al.*, "Prediction of multipactor breakdown thresholds in coaxial transmission lines for traveling, standing, and mixed waves," *IEEE Trans. Plasma Sci.*, vol. 37, no. 10, pp. 2031–2040, Oct. 2009.
[5] V. E. Semenov, E. I. Rakova, D. Anderson, M. Lisak, and J. Puech, "Multipactor in rectangular waveguides," *Phys. Plasmas*, vol. 14, no. 3, p. 033501, 2007.
[6] V. E. Semenov, N. A. Zharova, D. Anderson, M. Lisak, and J. Puech, "Simulations of multipactor in circular waveguides," *Phys. Plasmas*, vol. 17, no. 12, p. 123503, 2010.
[7] A. Coves, G. Torregrosa-Penalva, C. Vicente, B. Gimeno, and V. E. Boria, "Multipactor discharges in parallel-plate dielectric-loaded waveguides including space-charge effects," *IEEE Trans. Electron Devices*, vol. 55, no. 9, pp. 2505–2511, Sep. 2008.
[8] L. K. Ang, Y. Y. Lau, R. A. Kishek, and M. Gilgenbach, "Power deposited on a dielectric by multipactor," *IEEE Trans. Plasma Sci.*, vol. 26, no. 3, pp. 290–295, Jun. 1998.
[9] R. A. Kishek, Y. Y. Lau, L. K. Ang, A. Valfells, and R. M. Gilgenbach, "Multipactor discharge on metals and dielectrics: Historical review and recent theories," *Phys. Plasmas*, vol. 5, no. 5, p. 2120, May 1998.
[10] V. E. Semenov *et al.*, "Preliminary results on the multipactor effect prediction in RF components with ferrites," in *Proc. 14th IEEE Int. Vac. Electron. Conf. (IVEC)*, May 2013, pp. 1–2.
[11] D. González-Iglesias, B. Gimeno, V. E. Boria, A. Gómez, and A. Vegas, "Multipactor effect in a parallel-plate waveguide partially filled with magnetized ferrite," *IEEE Trans. Electron Devices*, vol. 61, no. 7, pp. 2552–2557, Jul. 2014.
[12] R. L. Geng, H. Padamsee, S. Belomestnykh, P. Goudket, D. M. Dykes, and R. G. Carter, "Suppression of multipacting in rectangular coupler waveguides," *Nucl. Instrum. Methods Phys. Res. A*, vol. 508, no. 3, pp. 227–238, 2003.
[13] V. E. Semenov *et al.*, "Reduction of the multipactor threshold due to electron cyclotron resonance," *IEEE Trans. Plasma Sci.*, vol. 40, no. 11, pp. 3062–3069, Nov. 2012.
[14] M. David Pozar, *Microwave Engineering*, 4th ed. New York, NY, USA: Wiley, 2012.
[15] A. J. B. Fuller, *Ferrites at Microwave Frequencies* (IEE Electromagnetic Waves Series). London, U.K.: IET, 2008, p. 280.
[16] J. Helszajn, *Waveguide Junction Circulators Theory and Practice*. New York, NY, USA: Wiley, 1998.
[17] R. E. Collin, *Foundations for Microwave Engineering*. 2nd ed. New York, NY, USA: McGraw-Hill, 1992.
[18] S. Anza, C. Vicente, D. Raboso, J. Gil, B. Gimeno, and V. E. Boria, "Enhanced prediction of multipaction breakdown in passive waveguide components including space charge effects," in *IEEE MTT-S Int. Microw. Symp. Dig.*, Jun. 2008, pp. 1095–1098.
[19] R. M. Vaughan, "Secondary emission formulas," *IEEE Trans. Electron Devices*, vol. 40, no. 4, p. 830, Apr. 1993.
[20] J. Greenwood, "The correct and incorrect generation of a cosine distribution of scattered particles for Monte-Carlo modelling of vacuum systems," *Vacuum*, vol. 67, no. 2, pp. 217–222, Sep. 2002.
[21] S. A. Schelkunoff, "Generalized telegraphist's equations for waveguides," *Bell Labs Tech. J.*, vol. 31, no. 4, pp. 784–801, Jul. 1952.
[22] A. Gómez, J. S. Ipiña M. A. Solano, A. Prieto, and A. Vegas, "Improving the coupled-mode method by means of step functions: Application to partial-height isotropic or anisotropic dielectric parallel-plate waveguides," *Microw. Opt. Techn. Lett.*, vol. 33, no. 6, pp. 408–414, Jun. 2002.

[23] A. Gómez, A. Lakhtakia, A. Vegas, and M. A. Solano, "Hybrid technique for analysing metallic waveguides containing isotropic chiral materials," *IET Microw. Antennas Propag.*, vol. 4, no. 3, pp. 305–315, Mar. 2010.
[24] I. Montero, F. Caspers, L. Aguilera, L. Galán, D. Raboso, and E. Montesinos, "Low-secondary electron yield of ferromagnetic materials and magnetized surfaces," in *Proc. IPAC*, Kyoto, Japan, May 2010, pp. 23–28.

Daniel González-Iglesias received the Licenciado degree in physics and the master's degree in advanced physics from the Universidad de Valencia, Valencia, Spain, in 2010 and 2011, respectively, where he is currently pursuing the Ph.D. degree in physics.

His current research interests include multipacting simulation of RF high-power passive components.

Álvaro Gómez was born in Santander, Spain, in 1976. He received the Licenciado en Ciencias Físicas and Ph.D. degrees from the Universidad de Cantabria, Santander, Spain, in 2000 and 2005, respectively.

He joined the Departamento de Ingeniería de Comunicaciones, Universidad de Cantabria, in 2000, where he became a Profesor Contratado Doctor in 2011. His current research interests include electromagnetic propagation in complex materials and numerical methods in electromagnetics.

Benito Gimeno (M'01) received the Licenciado degree in physics and the Ph.D. degree from the Universidad de Valencia, Valencia, Spain, in 1987 and 1992, respectively.

He became a Full Professor with the Universidad de Valencia in 2010. His current research interests include the electromagnetic analysis and design of microwave passive components and RF breakdown high-power effects.

Óscar Fernández was born in Santander, Spain, in 1976. He received the Degree in telecommunications engineering and the Ph.D. degree from the University of Cantabria, Santander, in 2001 and 2007, respectively. He joined the Department of Communication Engineering, University of Cantabria, in 2001. His current research interests include numerical methods in electromagnetism and microwave measurements.

Angel Vegas (M'98) received the Ph.D. degree in physical sciences from the University of Cantabria, Santander, Spain, in 1983.

He is currently a Full Professor of Electromagnetics with the University of Cantabria, where he is the Head of the Electromagnetics Group. His current research interests include the electromagnetics of complex materials, computer methods in electromagnetism, and microwave measurements.

Fernando Casas received the Ph.D. degree in theoretical physics from the University of Valencia, Valencia, Spain, in 1992.

He has been a Professor of Applied Mathematics with the Universitat Jaume I, Castellon, Spain, since 2009. His current research interests include geometric numerical integration, including the design and analysis of splitting and composition methods for differential equations and their applications, Lie group methods, perturbation techniques, and the algebraic issues involved.

Sergio Anza Hormigo received the B.S. degree in telecommunications engineering and the Ph.D. degree from the Universidad Politecnica de Valencia, Valencia, Spain.

He is currently with Aurora Software and Testing SL, Valencia. His current research interests include the areas of theory and numerical techniques for the modelling and prediction of nonlinear phenomena in RF high power devices for space applications.

Carlos Vicente (M'08) received the Diploma degree in physics from the Universidad de Valencia, Valencia, Spain, in 1999, and the Dr.Ing. degree in engineering from the Technical University of Darmstadt, Darmstadt, Germany, in 2005.

In 2006, he co-founded Aurora Software and Testing SL, Valencia, which is devoted to telecommunications sector. His research concerns the analysis and design of passive components for communications satellites with a special emphasis on high-power practical aspects.

Jordi Gil received the Licenciado degree in physics from the Universidad de Valencia, Valencia, Spain, in 2000, and the Ph.D. degree in telecommunications engineering from the Universidad Politécnica de Valencia, Valencia, in 2010.

In 2006, he co-founded Aurora Software and Testing SL, Valencia, which is devoted to the space sector. His current research interests include numerical methods in computer-aided techniques for the analysis and design of microwave passive components.

Rafael Mata received the Degree in physics and the Ph.D. degree from the Universidad de Valencia, Valencia, Spain, in 2006 and 2011, respectively.

He held a researcher/technician position with the Val Space Consortium, Valencia, in 2012. His current research interests include secondary electron emission properties, outgassing, and venting processes in RF high power space materials.

Isabel Montero is currently a Research Professor with the Spanish National Research Council (CSIC), Madrid, Spain. She is the Head of the Group Surface Nanostructuring for Space and Terrestrial Communications, Materials Science Institute of Madrid (ICMM-CSIC), Madrid. She is also the Director of Spanish Laboratory on secondary electron emission, CSIC.

Vicente E. Boria (S'91–A'99–SM'02) received the Doctor Ingeniero de Telecomunicación degree from the Universidad Politécnica de Valencia, Valencia, Spain, in 1997.

He is currently a Full Professor with the Universidad Politécnica de Valencia. His research interests include the electromagnetic analysis and design of microwave passive components and also RF breakdown high-power effects.

David Raboso received the Degree in physics from the Autonomous University of Madrid, Madrid, Spainand the master's degree in space engineering from the University of Delft, Delft, The Netherlands.

In 1992, he joined the European Space Agency, The Netherlands, where he became responsible for all activities related to RF breakdown in space microwave components. He has co-authored over 100 articles in prestigious journals and a Co-Inventor of nine patents.